ELSEVIER

Electrical Power and Energy Systems 25 (2003) 501–513

ELECTRICAL POWER & ENERGY SYSTEMS

www.elsevier.com/locate/ijepes

Review

Improved representation of control adjustments into the Newton–Raphson power flow

Abilio Manuel Variz[a], Vander Menengoy da Costa[a], José Luiz R. Pereira[a,*], Nelson Martins[b]

[a]*Faculdade de Engenharia, Campus da UFJF, Brazil*
[b]*CEPEL, P.O. Box 68007, CEP 21944-970, Rio de Janeiro, RJ, Brazil*

Abstract

This paper describes a sparse $(4n \times 4n)$ formulation for the solution of power flow problem, comprising $2n$ current injection equations written in rectangular coordinates plus the set of control equations. This formulation has the same convergence characteristics of the conventional Newton power flow problem, expressed in terms of power mismatches written in polar coordinates and can be reduced to a $(2n \times 2n)$ formulation plus the control equations. It is best suited to the incorporation of flexible AC transmission system devices and controls of any kind. Complex user-defined control functions, involving the participation of several regulating devices, can be directly introduced as power flow control data. The results presented validate the proposed method.

Keywords: Power flow; Power flow controls; Flexible AC transmission system devices

1. Introduction

The power flow problem deals with solving the set of non-linear algebraic equations which represent the network under steady state conditions. Over the last years, many algorithms have been developed regarding voltage stability tools [1–3], more advanced solution techniques [4] and the representation of both the more realistic modeling of power system components [5] and the recent technology devices [6,7].

In Ref. [5] is presented a static model for synchronous generators with voltage dependent reactive power limits due to the maximum stator current, maximum and minimum rotor current as well as maximum rotor angle limiters. This generator model is included in an ordinary power flow program.

In Ref. [6] is discussed the modeling of flexible AC transmission system (FACTS) devices for power flow studies and the role of that modeling in the study of FACTS devices for power flow control. Three generic types of FACTS devices are suggested and the integration of those devices into power flow studies is illustrated.

Generalized nodal admittance models are presented in Ref. [7] for series compensators, phase shifters interphase power controllers and unified power flow controllers, regarding to the insertion in a Newton–Raphson power flow program.

In Ref. [8] is presented a new procedure for the solution of power flow problem, by using the current injection equations written in rectangular coordinates. From this formulation it is possible to obtain the same convergence characteristics of the conventional power flow expressed in terms of power mismatches and written in polar coordinates. The set of controls and devices studied in Ref. [8] includes the representation of the voltage dependent load, load tap changing transformer and phase shifter transformer.

In Ref. [9] the static var compensator (SVC) is represented by adding a fictitious *PV* bus to the system with a fixed voltage equal to the SVC reference voltage. This fictitious bus is connected to the physical SVC-bus through a slope reactance.

The objective of this paper is to incorporate other control devices, by using the augmented formulation presented in Ref. [8]. The set of control devices studied includes the representation of *P* (only active power specified) and *PQV* (load bus in which the voltage is remotely controlled) buses,

* Corresponding author. Tel.: +55-32-3229-3444; fax: +55-32-3229-3401.

E-mail addresses: jluiz@ieee.org (J.L.R. Pereira), jluiz@lacee.ufjf.br (J.L.R. Pereira), abilio@lacee.ufjf.br (A.M. Variz), vandermcosta@uol.com.br (V.M. da Costa), nelson@cepel.br (N. Martins).

0142-0615/03/$ - see front matter © 2003 Elsevier Science Ltd. All rights reserved.
PII: S0142-0615(02)00126-6

Nomenclature

n	number of buses
h	iteration counter
$\Delta P_k + \mathrm{j}\Delta Q_k$	complex power mismatch at bus k
$P_{G_{(k)}} + \mathrm{j}Q_{G_{(k)}}$	generated complex power at bus k
$P_{L_{(k)}} + \mathrm{j}Q_{L_{(k)}}$	complex load at bus k
$P_k + \mathrm{j}Q_k$	net complex injected power at bus k
$P_k^{\mathrm{calc}} + \mathrm{j}Q_k^{\mathrm{calc}}$	calculated complex power at bus k
$V_{r_k} + \mathrm{j}V_{m_k}$	complex voltage at bus k
θ_k, V_k	voltage angle and magnitude at bus k
$G_{kj} + \mathrm{j}B_{kj}$	(k,j)th element of bus admittance matrix
$\Delta\theta$, ΔV	voltage angle and magnitude corrections
$r_{kj} + \mathrm{j}x_{kj}$	series impedance of line $(k-j)$
a_{kj}	transformer tap from bus k to bus j
y_{kj}	series admittance of line $(k-j)$
δ_k	load angle associated to the bus k
x_q	quadrature-axis synchronous reactance

static var compensators, thyristor controlled series compensation (TCSC) and reactive limits at a generation bus. User-defined control functions involving the participation of a combination of these devices can be incorporated into the power flow model.

2. The augmented formulation

The augmented formulation uses current injection equations expressed in terms of rectangular coordinates of voltage buses, for both *PQ* and *PV* buses [8]. The calculation of real and imaginary current mismatches is straightforward for *PQ* buses, because of real and reactive power mismatches are known. For *PV* buses the reactive power mismatch is unknown and it is treated in this formulation as a dependent variable. Then an additional equation is introduced in order to set the over-determination of the system of equations as follows:

$$V_k^2 = V_{r_k}^2 + V_{m_k}^2 \tag{1}$$

By linearizing Eq. (1) yields:

$$\Delta V_k = \frac{V_{r_k}}{V_k}\Delta V_{r_k} + \frac{V_{m_k}}{V_k}\Delta V_{m_k} \tag{2}$$

Thus, for each *PV* bus there are three equations and variables ΔV_{r_k}, ΔV_{r_m} and ΔQ_k.

The voltage angle at a bus k can be expressed by:

$$\theta_k = tg^{-1}\frac{V_{m_k}}{V_{r_k}} \tag{3}$$

Whose linearized form is:

$$\Delta\theta_k = \frac{V_{r_k}}{V_k^2}\Delta V_{m_k} - \frac{V_{m_k}}{V_k^2}\Delta V_{r_k} \tag{4}$$

The mathematical model is then written in the following matrix form [8]:

$$\begin{bmatrix} \underline{\mathbf{0}} \\ \underline{\mathbf{\Delta}}_{\theta V} \end{bmatrix} = \begin{bmatrix} \mathbf{Y}^* & \mathbf{B} \\ \mathbf{C} & \mathbf{0} \end{bmatrix} \begin{bmatrix} \underline{\mathbf{\Delta}}\mathbf{V}_{rm} \\ \underline{\mathbf{\Delta}}_{PQ} \end{bmatrix} \tag{5}$$

The $\mathbf{Y}^*$ matrix blocks have the following structure:

$$\mathbf{Y}_{kk}^* = \begin{bmatrix} B'_{kk} & G'_{kk} \\ G''_{kk} & B''_{kk} \end{bmatrix} \qquad \mathbf{Y}_{km}^* = \begin{bmatrix} B_{km} & G_{km} \\ G_{km} & -B_{km} \end{bmatrix}$$

$$B'_{kk} = B_{kk} - a_k \tag{6}$$

$$G'_{kk} = G_{kk} - b_k \tag{7}$$

$$G''_{kk} = G_{kk} - c_k \tag{8}$$

$$B''_{kk} = -B_{kk} - d_k \tag{9}$$

The parameters a_k, b_k, c_k and d_k are presented in Appendix A of Ref. [8].

The matrices **B** and **C** have a block-diagonal structure

$$\mathbf{B} = \begin{bmatrix} \mathbf{B}_1 & & & \\ & \mathbf{B}_2 & & \\ & & \ddots & \\ & & & \mathbf{B}_n \end{bmatrix} \qquad \mathbf{C} = \begin{bmatrix} \mathbf{C}_1 & & & \\ & \mathbf{C}_2 & & \\ & & \ddots & \\ & & & \mathbf{C}_n \end{bmatrix}$$

where:

$$\mathbf{B}_i = \begin{bmatrix} \frac{-V_{m_i}}{V_i^2} & \frac{V_{r_i}}{V_i^2} \\ \frac{-V_{r_i}}{V_i^2} & \frac{-V_{m_i}}{V_i^2} \end{bmatrix} \quad \mathbf{C}_i = \begin{bmatrix} \frac{-V_{m_i}}{V_i^2} & \frac{V_{r_i}}{V_i^2} \\ \frac{V_{r_i}}{V_i} & \frac{V_{m_i}}{V_i} \end{bmatrix}$$

$$\underline{\mathbf{\Delta}}_{\theta V} = [\Delta\theta_1 \;\; \Delta V_1 \;\; \Delta\theta_2 \;\; \Delta V_2 \;\; \cdots \;\; \Delta\theta_n \;\; \Delta V_n]^{\mathrm{t}}$$

$$\underline{\mathbf{\Delta}}_{PQ} = [\Delta P_1 \;\; \Delta Q_1 \;\; \Delta P_2 \;\; \Delta Q_2 \;\; \cdots \;\; \Delta P_n \;\; \Delta Q_n]^{\mathrm{t}}$$

$$\underline{\mathbf{\Delta}}\mathbf{V}_{rm} = [\Delta V_{r_1} \;\; \Delta V_{m_1} \;\; \Delta V_{r_2} \;\; \Delta V_{m_2} \;\; \cdots \;\; \Delta V_{r_n} \;\; \Delta V_{m_n}]^{\mathrm{t}}$$

The voltage buses updates are given by:

$$\underline{\mathbf{\Delta}}_{\theta V}^{(h)} = \mathbf{C}^{(h)} \underline{\mathbf{\Delta}}\mathbf{V}_{rm}^{(h)} \tag{10}$$

The new solution is given by:

$$\underline{\mathbf{V}}^{(h+1)} = \underline{\mathbf{V}}^{(h)} + \underline{\mathbf{\Delta}}\mathbf{V}^{(h)} \tag{11}$$

$$\underline{\boldsymbol{\theta}}^{(h+1)} = \underline{\boldsymbol{\theta}}^{(h)} + \underline{\mathbf{\Delta}}\boldsymbol{\theta}^{(h)} \tag{12}$$

As shown in Ref. [8], the step 1 of the solution algorithm for $(4n \times 4n)$ augmented formulation is equivalent to $(2n \times 2n)$ formulation plus control equations.

3. Remote voltage control and secondary voltage control models

A generation bus (P bus) can be used to control the voltage at a remote bus (PQV bus) by assuming the voltage at the P bus as the unknown and specifying the voltage at the PQV bus. In this case, the voltage constraint equation related to the PQV bus must be included into the Jacobian matrix.

On the other hand, if various P buses (say NP) are assumed to control a single PQV bus voltage, then $(NP - 1)$ additional equations are required to yield a unique solution, where each equation describes the MVAr participation factors among the P buses, as follows

$$Q_{\mathrm{G}_{(i)}} - \alpha_k Q_{\mathrm{G}_{(j)}} = 0 \tag{13}$$

where i and j denote P buses, $k = 1, 2, \ldots, (NP - 1)$

$$Q_{\mathrm{G}_{(i)}} = Q_i + Q_{\mathrm{L}_{(i)}} \tag{14}$$

Thus, Eq. (13) is linearized as shown below:

$$\Delta Q' = \Delta Q_{(i)} - \alpha_k \Delta Q_{(j)} \tag{15}$$

where:

$$\Delta Q' = Q_{\mathrm{L}_{(i)}} + \alpha_k Q_{\mathrm{L}_{(j)}} - (Q_i^{\mathrm{calc}} - \alpha_k Q_j^{\mathrm{calc}}) \tag{16}$$

The augmented system of equations is then modified to incorporate Eq. (16). In addition, the voltage constraint equation for the PQV bus must be introduced

$$\begin{bmatrix} \underline{\mathbf{0}} \\ \underline{\mathbf{\Delta}}_{\theta V} \\ \underline{\mathbf{\Delta}}\mathbf{Q}' \end{bmatrix} = \begin{bmatrix} \mathbf{Y}^* & \mathbf{B} \\ \mathbf{C} & \mathbf{D} \end{bmatrix} = \begin{bmatrix} \underline{\mathbf{\Delta}}\mathbf{V}_{rm} \\ \underline{\mathbf{\Delta}}_{PQ} \end{bmatrix} \tag{17}$$

where:

$$\mathbf{D} = \begin{bmatrix} \mathbf{D}_1 \\ \mathbf{D}_2 \\ \vdots \\ \mathbf{D}_n \end{bmatrix}$$

For all PQ, PV and PQV buses:

$$\mathbf{D}_k = [\mathbf{0}]$$

For remote voltage control (only one P bus i) one has:

$$\mathbf{C}_i = \begin{bmatrix} \frac{-V_{m_i}}{V_i^2} & \frac{V_{r_i}}{V_i^2} \\ \frac{V_{r_l}}{V_l} & \frac{V_{m_l}}{V_l} \end{bmatrix} \quad \mathbf{D}_i = \begin{bmatrix} \cdots & 0 & \cdots & 0 & \cdots \\ \cdots & 0 & \cdots & 0 & \cdots \end{bmatrix}$$

For secondary voltage control ($NP - 1$ P buses j) one has

$$\mathbf{C}_j = \begin{bmatrix} \frac{-V_{m_j}}{V_j^2} & \frac{V_{r_j}}{V_j^2} \\ 0 & 0 \end{bmatrix} \quad \mathbf{D}_j = \begin{bmatrix} \cdots & 0 & \cdots & 0 & \cdots \\ \cdots & 1 & \cdots & -\alpha_k & \cdots \end{bmatrix}$$

where l denotes PQV bus and the non-zero values in matrix $\mathbf{D}_j$ occur in the columns i and j.

3.1. Illustration example

3.1.1. Remote voltage control by a single reactive source

In Fig. 1 suppose the voltage at bus 2 is remotely controlled by reactive power at bus 4, and bus 3 is assumed to be a PQ bus type. Bus 1 is the slack bus. The linear system of equations related to the solution algorithm step 1,

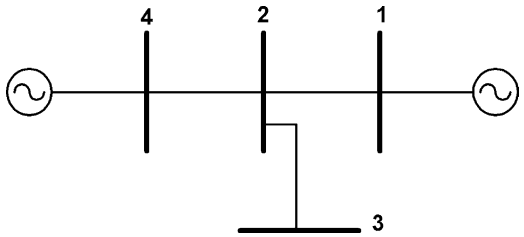

Fig. 1. Four-bus test system.

presented in Ref. [8], is given by Eq. (18).

$$\begin{bmatrix} 0 \\ 0 \\ 0 \\ \Delta P_2 \\ \Delta Q_2 \\ 0 \\ 0 \\ \Delta P_3 \\ \Delta Q_3 \\ 0 \\ 0 \\ \Delta P_4 \\ 0 \end{bmatrix} = \begin{bmatrix} B'_{22} & G'_{22} & \frac{-V_{m_2}}{V_2^2} & \frac{V_{r_2}}{V_2^2} & B_{23} & G_{23} & 0 & 0 & B_{24} & G_{24} & 0 & 0 \\ G''_{22} & B''_{22} & \frac{-V_{r_2}}{V_2^2} & \frac{-V_{m_2}}{V_2^2} & G_{23} & -B_{23} & 0 & 0 & G_{24} & -B_{24} & 0 & 0 \\ 0 & 0 & 1 & 0 & 0 & 0 & 0 & 0 & 0 & 0 & 0 & 0 \\ 0 & 0 & 0 & 1 & 0 & 0 & 0 & 0 & 0 & 0 & 0 & 0 \\ B_{32} & G_{32} & 0 & 0 & B'_{33} & G'_{33} & \frac{-V_{m_3}}{V_3^2} & \frac{V_{r_3}}{V_3^2} & & & & \\ G_{32} & -B_{32} & 0 & 0 & G''_{33} & B''_{33} & \frac{-V_{r_3}}{V_3^2} & \frac{-V_{m_3}}{V_3^2} & & & & \\ 0 & 0 & 0 & 0 & 0 & 0 & 1 & 0 & & & & \\ 0 & 0 & 0 & 0 & 0 & 0 & 0 & 1 & & & & \\ B_{42} & G_{42} & 0 & 0 & & & & & B'_{44} & G'_{44} & \frac{-V_{m_4}}{V_4^2} & \frac{V_{r_4}}{V_4^2} \\ G_{42} & -B_{42} & 0 & 0 & & & & & G''_{44} & B''_{44} & \frac{-V_{r_4}}{V_4^2} & \frac{-V_{m_4}}{V_4^2} \\ 0 & 0 & 0 & 0 & & & & & 0 & 0 & 1 & 0 \\ \frac{V_{r_2}}{V_2} & \frac{V_{m_2}}{V_2} & 0 & 0 & & & & & 0 & 0 & 0 & 0 \end{bmatrix} \begin{bmatrix} \Delta V_{r_2} \\ \Delta V_{m_2} \\ \Delta P_2 \\ \Delta Q_2 \\ \Delta V_{r_3} \\ \Delta V_{m_3} \\ \Delta P_3 \\ \Delta Q_3 \\ \Delta V_{r_4} \\ \Delta V_{m_4} \\ \Delta P_4 \\ \Delta Q_4 \end{bmatrix} \tag{18}$$

3.1.2. Remote voltage control by multiple reactive sources

Now, assume the reactive power sources at buses 3 and 4 are supposed to control the voltage at bus 2. In this case, the participation factor, which establishes the relationship between the reactive power sources must be specified, leading to:

$$Q_{G_{(3)}} = \alpha_1 Q_{G_{(4)}} \tag{19}$$

The linear system of equations related to the solution algorithm step 1, presented in Ref. [8], is given by Eq. (21), where:

$$\Delta Q'''_1 = -Q_{L_{(3)}} + \alpha_1 Q_{L_{(4)}} \tag{20}$$

$$\begin{bmatrix} 0 \\ 0 \\ \Delta P_2 \\ \Delta Q_2 \\ 0 \\ 0 \\ \Delta P_3 \\ 0 \\ 0 \\ 0 \\ \Delta P_4 \\ \Delta Q'''_1 \end{bmatrix} = \begin{bmatrix} B'_{22} & G'_{22} & \frac{-V_{m_2}}{V_2^2} & \frac{V_{r_2}}{V_2^2} & B_{23} & G_{23} & 0 & 0 & B_{24} & G_{24} & 0 & 0 \\ G''_{22} & B''_{22} & \frac{-V_{r_2}}{V_2^2} & \frac{-V_{m_2}}{V_2^2} & G_{23} & -B_{23} & 0 & 0 & G_{24} & -B_{24} & 0 & 0 \\ 0 & 0 & 1 & 0 & 0 & 0 & 0 & 0 & 0 & 0 & 0 & 0 \\ 0 & 0 & 0 & 1 & 0 & 0 & 0 & 0 & 0 & 0 & 0 & 0 \\ B_{32} & G_{32} & 0 & 0 & B'_{33} & G'_{33} & \frac{-V_{m_3}}{V_3^2} & \frac{V_{r_3}}{V_3^2} & & & & \\ G_{32} & -B_{32} & 0 & 0 & G''_{33} & B''_{33} & \frac{-V_{r_3}}{V_3^2} & \frac{-V_{m_3}}{V_3^2} & & & & \\ 0 & 0 & 0 & 0 & 0 & 0 & 1 & 0 & & & & \\ \frac{V_{r_2}}{V_2} & \frac{V_{m_2}}{V_2} & 0 & 0 & 0 & 0 & 0 & 0 & & & & \\ B_{42} & G_{42} & 0 & 0 & & & & & B'_{44} & G'_{44} & \frac{-V_{m_4}}{V_4^2} & \frac{V_{r_4}}{V_4^2} \\ G_{42} & -B_{42} & 0 & 0 & & & & & G''_{44} & B''_{44} & \frac{-V_{r_4}}{V_4^2} & \frac{-V_{m_4}}{V_4^2} \\ 0 & 0 & 0 & 0 & & & & & 0 & 0 & 1 & 0 \\ 0 & 0 & 0 & 0 & 0 & 0 & 0 & 1 & 0 & 0 & 0 & -\alpha_1 \end{bmatrix} \begin{bmatrix} \Delta V_{r_2} \\ \Delta V_{m_2} \\ \Delta P_2 \\ \Delta Q_2 \\ \Delta V_{r_3} \\ \Delta V_{m_3} \\ \Delta P_3 \\ \Delta Q_3 \\ \Delta V_{r_4} \\ \Delta V_{m_4} \\ \Delta P_4 \\ \Delta Q_4 \end{bmatrix} \tag{21}$$

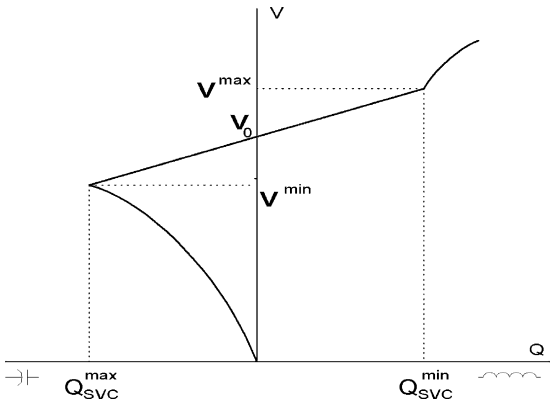

Fig. 2. Voltage × reactive power characteristic.

4. The static var compensator model

The steady state voltage × reactive power characteristics for an SVC is shown in Fig. 2. The linear control range lies within the limits determined by the maximum susceptance of the reactor and the total susceptance determined by the capacitor banks in service and the filter capacitance [10,11].

Within the linear control range the SVC is equivalent to a voltage source in series with a slope reactance X_s as follows

$$V_k = V_0 + X_s I_k \tag{22}$$

where k denotes the bus at which the SVC is installed.

From Fig. 2

$$V_k = V_0 + r_k Q_{G_{(k)}} \tag{23}$$

where:

$$V_0 = \frac{V_k^{\max} Q_{G_{(k)}}^{\max} - V_k^{\min} Q_{G_{(k)}}^{\min}}{Q_{G_{(k)}}^{\max} - Q_{G_{(k)}}^{\min}} \tag{24}$$

$$r_k = \frac{V_k^{\min} - V_k^{\max}}{Q_{G_{(k)}}^{\max} - Q_{G_{(k)}}^{\min}} \tag{25}$$

For $Q_{G_{(k)}} > Q_{G_{(k)}}^{\max}$ the SVC behaves as a capacitor and the corresponding reactive power is given by:

$$Q_{G_{(k)}} = \frac{Q_{G_{(k)}}^{\max}}{(V_k^{\min})^2} V_k^2 \tag{26}$$

For $Q_{G_{(k)}} < Q_{G_{(k)}}^{\min}$ the SVC behaves as a reactor and the corresponding reactive power is given by:

$$Q_{G_{(k)}} = \frac{Q_{G_{(k)}}^{\min}}{(V_k^{\max})^2} V_k^2 \tag{27}$$

Eqs. (23), (26) and (27) are linearized and the voltages are expressed in rectangular coordinates. Thus, Eq. (23) leads to

$$\Delta V_k' = \frac{V_{r_k}}{V_k}\Delta V_{r_k} + \frac{V_{m_k}}{V_k}\Delta V_{m_k} + r_k \Delta Q_k \tag{28}$$

where:

$$\Delta V_k' = V_0 + r_k(Q_{L_{(k)}} + Q_k) - V_k \tag{29}$$

Eq. (26) leads to

$$\Delta Q_k' \max = 2\frac{Q_{G_{(k)}}^{\max}}{(V_k^{\min})^2} V_{rk}\Delta V_{rk} + 2\frac{Q_{G_{(k)}}^{\max}}{(V_k^{\min})^2} V_{m_k}\Delta V_{m_k} - \Delta Q_k \tag{30}$$

where:

$$\Delta Q_k'^{\max} = Q_{L_{(k)}} + Q_k - \frac{Q_{G_{(k)}}^{\max}}{(V_k^{\min})^2} V_k^2 \tag{31}$$

Eq. (27) leads to

$$\Delta Q_k'^{\min} = 2\frac{Q_{G_{(k)}}^{\min}}{(V_k^{\max})^2} V_{r_k}\Delta V_{r_k} + 2\frac{Q_{G_{(k)}}^{\min}}{(V_k^{\max})^2} V_{m_k}\Delta V_{m_k} - \Delta Q_k \tag{32}$$

where:

$$\Delta Q_k'^{\min} = Q_{L_{(k)}} + Q_k - \frac{Q_{G_{(k)}}^{\min}}{(V_k^{\max})^2} V_k^2 \tag{33}$$

The implementation procedure is similar to that used for the *PV* bus. Instead of using the voltage constraint equation, either one of Eqs. (28), (30) and (32) is used depending on the SVC operating point.

4.1. Illustration example

In Fig. 3, suppose a SVC connected at bus 3 to control the voltage at bus 2, say V_2^{sp}. The linear system of equations

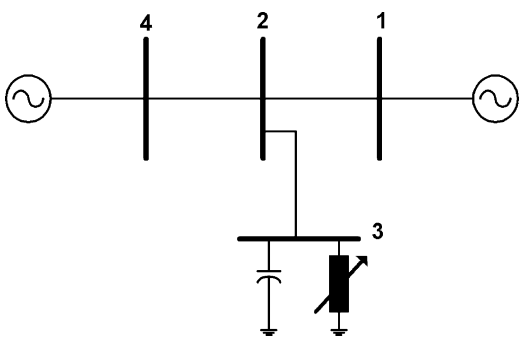

Fig. 3. Topology for incorporation of SVC.

related to the solution algorithm step 1, presented in Ref. [8], is given by:

$$
\begin{bmatrix} 0 \\ 0 \\ \Delta P_2 \\ \Delta Q_2 \\ 0 \\ 0 \\ \Delta P_3 \\ \Delta V_2' \\ 0 \\ 0 \\ \Delta P_4 \\ 0 \end{bmatrix} =
\begin{bmatrix}
B_{22}' & G_{22}' & \frac{-V_{m_2}}{V_2^2} & \frac{V_{r_2}}{V_2^2} & B_{23} & G_{23} & 0 & 0 & B_{24} & G_{24} & 0 & 0 \\
G_{22}'' & B_{22}'' & \frac{-V_{r_2}}{V_2^2} & \frac{-V_{m_2}}{V_2^2} & G_{23} & -B_{23} & 0 & 0 & G_{24} & -B_{24} & 0 & 0 \\
0 & 0 & 1 & 0 & 0 & 0 & 0 & 0 & 0 & 0 & 0 & 0 \\
0 & 0 & 0 & 1 & 0 & 0 & 0 & 0 & 0 & 0 & 0 & 0 \\
B_{32} & G_{32} & 0 & 0 & B_{33}' & G_{33}' & \frac{-V_{m_3}}{V_3^2} & \frac{V_{r_3}}{V_3^2} & & & & \\
G_{32} & -B_{32} & 0 & 0 & G_{33}'' & B_{33}'' & \frac{-V_{r_3}}{V_3^2} & \frac{-V_{m_3}}{V_3^2} & & & & \\
0 & 0 & 0 & 0 & 0 & 0 & 1 & 0 & & & & \\
\frac{V_{r_2}}{V_2} & \frac{V_{m_2}}{V_2} & 0 & r_2 & 0 & 0 & 0 & 0 & & & & \\
B_{42} & G_{42} & 0 & 0 & & & & & B_{44}' & G_{44}' & \frac{-V_{m_4}}{V_4^2} & \frac{V_{r_4}}{V_4^2} \\
G_{42} & -B_{42} & 0 & 0 & & & & & G_{44}'' & B_{44}'' & \frac{-V_{r_4}}{V_4^2} & \frac{-V_{m_4}}{V_4^2} \\
0 & 0 & 0 & 0 & & & & & 0 & 0 & 1 & 0 \\
0 & 0 & 0 & 0 & & & & & \frac{V_{r_4}}{V_4} & \frac{V_{m_4}}{V_4} & 0 & 0
\end{bmatrix}
\begin{bmatrix} \Delta V_{r_2} \\ \Delta V_{m_2} \\ \Delta P_2 \\ \Delta Q_2 \\ \Delta V_{r_3} \\ \Delta V_{m_3} \\ \Delta P_3 \\ \Delta Q_3 \\ \Delta V_{r_4} \\ \Delta V_{m_4} \\ \Delta P_4 \\ \Delta Q_4 \end{bmatrix} \tag{34}
$$

If the SVC is operating as a capacitor, then the linear system of equations becomes

$$
\begin{bmatrix} 0 \\ 0 \\ \Delta P_2 \\ \Delta Q_2 \\ 0 \\ 0 \\ \Delta P_3 \\ \Delta Q_2^{'\max} \\ 0 \\ 0 \\ \Delta P_4 \\ 0 \end{bmatrix} =
\begin{bmatrix}
B_{22}' & G_{22}' & \frac{-V_{m_2}}{V_2^2} & \frac{V_{r_2}}{V_2^2} & B_{23} & G_{23} & 0 & 0 & B_{24} & G_{24} & 0 & 0 \\
G_{22}'' & B_{22}'' & \frac{-V_{r_2}}{V_2^2} & \frac{-V_{m_2}}{V_2^2} & G_{23} & -B_{23} & 0 & 0 & G_{24} & -B_{24} & 0 & 0 \\
0 & 0 & 1 & 0 & 0 & 0 & 0 & 0 & 0 & 0 & 0 & 0 \\
0 & 0 & 0 & 1 & 0 & 0 & 0 & 0 & 0 & 0 & 0 & 0 \\
B_{32} & G_{32} & 0 & 0 & B_{33}' & G_{33}' & \frac{-V_{m_3}}{V_3^2} & \frac{V_{r_3}}{V_3^2} & & & & \\
G_{32} & -B_{32} & 0 & 0 & G_{33}'' & B_{33}'' & \frac{-V_{r_3}}{V_3^2} & \frac{-V_{m_3}}{V_3^2} & & & & \\
0 & 0 & 0 & 0 & 0 & 0 & 1 & 0 & & & & \\
f_2 V_{r_2} & f_2 V_{m_2} & 0 & -1 & 0 & 0 & 0 & 0 & & & & \\
B_{42} & G_{42} & 0 & 0 & & & & & B_{44}' & G_{44}' & \frac{-V_{m_4}}{V_4^2} & \frac{V_{r_4}}{V_4^2} \\
G_{42} & -B_{42} & 0 & 0 & & & & & G_{44}'' & B_{44}'' & \frac{-V_{r_4}}{V_4^2} & \frac{-V_{m_4}}{V_4^2} \\
0 & 0 & 0 & 0 & & & & & 0 & 0 & 1 & 0 \\
0 & 0 & 0 & 0 & & & & & \frac{V_{r_4}}{V_4} & \frac{V_{m_4}}{V_4} & 0 & 0
\end{bmatrix}
\begin{bmatrix} \Delta V_{r_2} \\ \Delta V_{m_2} \\ \Delta P_2 \\ \Delta Q_2 \\ \Delta V_{r_3} \\ \Delta V_{m_3} \\ \Delta P_3 \\ \Delta Q_3 \\ \Delta V_{r_4} \\ \Delta V_{m_4} \\ \Delta P_4 \\ \Delta Q_4 \end{bmatrix} \tag{35}
$$

where:

$$f_k = 2\frac{Q_{G_{(k)}}^{\max}}{(V_k^{\min})^2} \tag{36}$$

5. Thyristor controlled series compensation model

The TCSC has both electromechanical stability and power flow control duties. In the latter case, it is used to regulate the power flow through a specified line. The TCSC control model studied here is referred to in the literature as constant line power control. Assume the TCSC is connected between buses k and j to control the active power flow P_{kj} through changes in the line reactance x_{kj}. Thus, the linearized equation of P_{kj} needs be introduced into the Jacobian matrix, as follows

$$\begin{bmatrix} \underline{\mathbf{0}} \\ \underline{\mathbf{\Delta}}_{\theta V} \\ \mathbf{\Delta}P_{kj} \end{bmatrix} \begin{bmatrix} \mathbf{Y}^{*} & \mathbf{B} & \underline{\mathbf{E}} \\ \mathbf{C} & \mathbf{0} & \underline{\mathbf{0}} \\ \underline{\mathbf{D}}^{\mathbf{t}} & \underline{\mathbf{0}}^{\mathbf{t}} & \mathbf{F} \end{bmatrix} \begin{bmatrix} \underline{\mathbf{\Delta}}\mathbf{V}_{r_m} \\ \underline{\mathbf{\Delta}}_{PQ} \\ \mathbf{\Delta}\mathbf{x}_{kj} \end{bmatrix} \tag{37}$$

where

$$\underline{\mathbf{D}} = \begin{bmatrix} \cdots & \dfrac{\partial P_{kj}}{\partial V_{r_k}} & \dfrac{\partial P_{kj}}{\partial V_{m_k}} & \cdots & \dfrac{\partial P_{kj}}{\partial V_{r_j}} & \dfrac{\partial P_{kj}}{\partial V_{m_j}} & \cdots \end{bmatrix}^{\mathrm{t}}$$

$$\underline{\mathbf{E}} = -\begin{bmatrix} \cdots & \dfrac{\partial \Delta I_{m_k}}{\partial x_{kj}} & \dfrac{\partial \Delta I_{r_k}}{\partial x_{k_j}} & \cdots & \dfrac{\partial \Delta I_{m_j}}{\partial x_{kj}} & \dfrac{\partial \Delta I_{r_j}}{\partial x_{kj}} & \cdots \end{bmatrix}^{\mathrm{t}}$$

$$\mathbf{F} = \frac{\partial P_{kj}}{\partial x_{kj}}$$

with

$$\frac{\partial \Delta I_{m_k}}{\partial x_{kj}} = \frac{2r_{kj}x_{kj}}{(r_{kj}^2+x_{kj}^2)^2}[-a_{kj}\cos(\varphi_{kj})V_{m_j} + a_{kj}\,sin(\varphi_{kj})V_{r_j} + a_{kj}^2 V_{m_k}] - \frac{r_{kj}^2-x_{kj}^2}{(r_{kj}^2+x_{kj}^2)^2}[a_{kj}\sin(\varphi_{kj})V_{m_j} + a_{kj}\cos(\varphi_{kj})V_{r_j} - a_{kj}^2 V_{r_k}] \tag{38}$$

$$\frac{\partial \Delta I_{r_k}}{\partial x_{kj}} = \frac{2r_{kj}x_{kj}}{(r_{kj}^2+x_{kj}^2)^2}[-a_{kj}\cos(\varphi_{kj})V_{r_j} - a_{kj}\sin(\varphi_{kj})V_{m_j} + a_{kj}^2 V_{r_k}] - \frac{r_{kj}^2-x_{kj}^2}{(r_{kj}^2+x_{kj}^2)^2}[a_{kj}\sin(\varphi_{kj})V_{r_j} - a_{kj}\cos(\varphi_{kj})V_{m_j} + a_{kj}^2 V_{m_k}] \tag{39}$$

$$\frac{\partial \Delta I_{m_j}}{\partial x_{kj}} = \frac{2r_{kj}x_{kj}}{(r_{kj}^2+x_{kj}^2)^2}[-a_{kj}\cos(\varphi_{kj})V_{m_k} - a_{kj}\sin(\varphi_{kj})V_{r_k} + V_{m_j}] - \frac{r_{kj}^2-x_{kj}^2}{(r_{kj}^2+x_{kj}^2)^2}[-a_{kj}\sin(\varphi_{kj})V_{m_k} + a_{kj}\cos(\varphi_{kj})V_{r_k} - V_{r_j}] \tag{40}$$

$$\frac{\partial \Delta I_{r_j}}{\partial x_{kj}} = \frac{2r_{kj}x_{kj}}{(r_{kj}^2+x_{kj}^2)^2}[a_{kj}\sin(\varphi_{kj})V_{m_k} - a_{kj}\cos(\varphi_{kj})V_{r_k} + V_{r_j}] - \frac{r_{kj}^2-x_{kj}^2}{(r_{kj}^2+x_{kj}^2)^2}[-a_{kj}\cos(\varphi_{kj})V_{m_k} - a_{kj}\sin(\varphi_{kj})V_{r_k} + V_{m_j}] \tag{41}$$

$$\frac{\partial \Delta P_{kj}}{\partial x_{kj}} = \frac{2r_{kj}x_{kj}a_{kj}}{(r_{kj}^2+x_{kj}^2)^2}[\cos(\varphi_{kj})(V_{r_k}V_{r_j}+V_{m_k}V_{m_j}) - \sin(\varphi_{kj}) \times (V_{m_k}V_{r_j} - V_{r_k}V_{m_j})] - \frac{2r_{kj}x_{kj}}{(r_{kj}^2+x_{kj}^2)^2}[a_{kj}^2(V_{r_k}^2+V_{m_k}^2)] + \frac{a_{kj}(r_{kj}^2-x_{kj}^2)}{(r_{kj}^2+x_{kj}^2)^2}[\cos(\varphi_{kj})(V_{m_k}V_{r_j} - V_{r_k}V_{m_j}) + \sin(\varphi_{kj})(V_{r_k}V_{r_j}+V_{m_k}V_{m_j})] \tag{42}$$

The line reactance value for the next iteration is given by:

$$x_{kj}^{(h+1)} = x_{kj}^{(h)} + \Delta x_{kj}^{(h)} \tag{43}$$

5.1. Illustration example

$$
\begin{bmatrix} 0 \\ 0 \\ \Delta P_2 \\ 0 \\ 0 \\ 0 \\ \Delta P_3 \\ \Delta Q_3 \\ 0 \\ 0 \\ \Delta P_4 \\ \Delta Q_4 \\ \Delta P_{34} \end{bmatrix} =
\begin{bmatrix}
B'_{22} & G'_{22} & \frac{-V_{m_2}}{V_2^2} & \frac{V_{r_2}}{V_2^2} & & & & & B_{24} & G_{24} & 0 & 0 & \\
G''_{22} & B''_{22} & \frac{-V_{r_2}}{V_2^2} & \frac{-V_{m_2}}{V_2^2} & & & & & G_{24} & -B_{24} & 0 & 0 & \\
0 & 0 & 1 & 0 & & & & & 0 & 0 & 0 & 0 & \\
\frac{V_{r_2}}{V_2} & \frac{V_{m_2}}{V_2} & 0 & 0 & & & & & 0 & 0 & 0 & 0 & \\
 & & & & B'_{33} & G'_{33} & \frac{-V_{m_3}}{V_3^2} & \frac{V_{r_3}}{V_3^2} & B_{34} & G_{34} & 0 & 0 & -\frac{\partial \Delta I_{m_3}}{\partial x_{34}} \\
 & & & & G''_{33} & B''_{33} & \frac{-V_{r_3}}{V_3^2} & \frac{-V_{m_3}}{V_3^2} & G_{34} & -B_{34} & 0 & 0 & -\frac{\partial \Delta I_{r_3}}{\partial x_{34}} \\
 & & & & 0 & 0 & 1 & 0 & 0 & 0 & 0 & 0 & 0 \\
 & & & & 0 & 0 & 0 & 1 & 0 & 0 & 0 & 0 & 0 \\
B_{42} & G_{42} & 0 & 0 & B_{43} & G_{43} & 0 & 0 & B'_{44} & G'_{44} & \frac{-V_{m_4}}{V_4^2} & \frac{V_{r_4}}{V_4^2} & -\frac{\partial \Delta I_{m_4}}{\partial x_{34}} \\
G_{42} & -B_{42} & 0 & 0 & G_{43} & -B_{43} & 0 & 0 & G''_{44} & B''_{44} & \frac{-V_{r_4}}{V_4^2} & \frac{-V_{m_4}}{V_4^2} & -\frac{\partial \Delta I_{r_4}}{\partial x_{34}} \\
0 & 0 & 0 & 0 & 0 & 0 & 0 & 0 & 0 & 0 & 1 & 0 & 0 \\
0 & 0 & 0 & 0 & 0 & 0 & 0 & 0 & 0 & 0 & 0 & 1 & 0 \\
 & & & & \frac{\partial \Delta P_{34}}{\partial V_{r_3}} & \frac{\partial \Delta P_{34}}{\partial V_{m_3}} & 0 & 0 & \frac{\partial \Delta P_{34}}{\partial V_{r_4}} & \frac{\partial \Delta P_{34}}{\partial V_{m_4}} & 0 & 0 & \frac{\partial \Delta P_{34}}{\partial x_{34}}
\end{bmatrix}
\begin{bmatrix} \Delta V_{r_2} \\ \Delta V_{m_2} \\ \Delta P_2 \\ \Delta Q_2 \\ \Delta V_{r_3} \\ \Delta V_{m_3} \\ \Delta P_3 \\ \Delta Q_3 \\ \Delta V_{r_4} \\ \Delta V_{m_4} \\ \Delta P_4 \\ \Delta Q_4 \\ \Delta x_{34} \end{bmatrix} \tag{44}
$$

In Fig. 4, suppose a TCSC connected between buses 3 and 4 to control the active power flow P_{34} at say, P_{34}^{sp}. The linear system of equations related to the solution algorithm step 1, presented in Ref. [8], is given by Eq. (44) where:

$$\Delta P_{34} = P_{34}^{sp} - P_{34}^{calc} \tag{45}$$

6. Reactive limits at a generation bus model

The model commonly used for power flow studies considers fixed reactive power limits for a synchronous generator. This is an approximation since the reactive power limits depend on the active power dispatch and the generator operating voltage. A realistic representation of the generator limits requires the determination of the capability diagram for the synchronous generator [5].

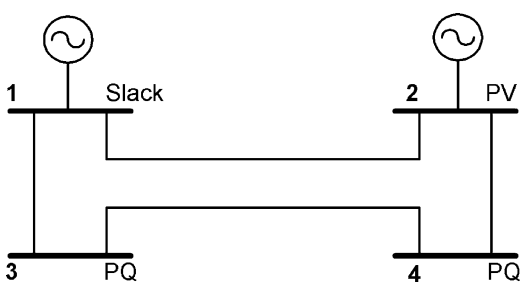

Fig. 4. Topology for TCSC control.

In Ref. [5] is represented the maximum and minimum limits for the reactive power generation taking into account the maximum stator current, the rotor current limiter and underexcitation limiter. Both salient pole and round rotor generators can be represented.

The proposal of this paper is to model the generation bus into a power flow program considering that the limits obtained for the reactive power generation are voltage dependent due to all the equipment limits modeled in Ref. [5]. When the reactive power generation of a machine connected at a bus k is within the range defined by the maximum and minimum limits, the following equation is introduced into the power flow program:

$$V_k = V_{nom} \tag{46}$$

On the other hand, if the reactive power generation is outside the limits, the following equation is introduced:

$$Q_{G_{(k)}} = Q_{lim} \tag{47}$$

where Q_{lim} is the maximum or minimum reactive power generation limits which is violated in a given iteration.

This value for a generation bus k is determined from the reactive power limits imposed by stator, rotor and underexcitation, given by Eqs. (48)–(50), respectively [5]:

$$Q_{\text{est}}^{(\max,\min)} = \pm\sqrt{(S_k^{\max})^2 - P_{G_{(k)}}^2} \tag{48}$$

$$Q_{\text{rot}}^{\max} = \frac{-V_k^2}{x_{q_{(k)}}} + \sqrt{\frac{V_k^2 (E_{q_{(k)}}^{\max})^2}{x_{q_{(k)}}^2} - P_{G_{(k)}}^2} \tag{49}$$

$$Q_{\text{exc}}^{\min} = \frac{P_{G_{(k)}}}{tg(\delta_k^{\max})} - \frac{V_k^2}{x_{q_{(k)}}} \tag{50}$$

Eqs. (46) and (47) are linearized and the voltages are expressed in rectangular coordinates. Thus, Eq. (46) leads to:

$$\Delta V_k'' = V_{\text{nom}} - V_k = \frac{V_{r_k}}{V_k}\Delta V_{r_k} + \frac{V_{m_k}}{V_k}\Delta V_{m_k} \tag{51}$$

Eq. (47) leads to:

$$\Delta Q_k'' = Q_{L_{(k)}} + Q_k - Q_{\text{lim}} = -\Delta Q_k \tag{52}$$

$$\begin{bmatrix} 0 \\ 0 \\ \Delta P_2 \\ \Delta Q_2 \\ 0 \\ 0 \\ \Delta P_3 \\ \Delta Q_3 \\ 0 \\ 0 \\ \Delta P_4 \\ \Delta V_2'' \end{bmatrix} = \begin{bmatrix} B_{22}' & G_{22}' & \frac{-V_{m_2}}{V_2^2} & \frac{V_{r_2}}{V_2^2} & B_{23} & G_{23} & 0 & 0 & B_{24} & G_{24} & 0 & 0 \\ G_{22}'' & B_{22}'' & \frac{-V_{r_2}}{V_2^2} & \frac{-V_{m_2}}{V_2^2} & G_{23} & -B_{23} & 0 & 0 & G_{24} & -B_{24} & 0 & 0 \\ 0 & 0 & 1 & 0 & 0 & 0 & 0 & 0 & 0 & 0 & 0 & 0 \\ 0 & 0 & 0 & 1 & 0 & 0 & 0 & 0 & 0 & 0 & 0 & 0 \\ B_{32} & G_{32} & 0 & 0 & B_{33}' & G_{33}' & \frac{-V_{m_3}}{V_3^2} & \frac{V_{r_3}}{V_3^2} & & & & \\ G_{32} & -B_{32} & 0 & 0 & G_{33}'' & B_{33}'' & \frac{-V_{r_3}}{V_3^2} & \frac{-V_{m_3}}{V_3^2} & & & & \\ 0 & 0 & 0 & 0 & 0 & 0 & 1 & 0 & & & & \\ 0 & 0 & 0 & 0 & 0 & 0 & 0 & 1 & & & & \\ B_{42} & G_{42} & 0 & 0 & & & & & B_{44}' & G_{44}' & \frac{-V_{m_4}}{V_4^2} & \frac{V_{r_4}}{V_4^2} \\ G_{42} & -B_{42} & 0 & 0 & & & & & G_{44}'' & B_{44}'' & \frac{-V_{r_4}}{V_4^2} & \frac{-V_{m_4}}{V_4^2} \\ 0 & 0 & 0 & 0 & & & & & 0 & 0 & 1 & 0 \\ 0 & 0 & 0 & 0 & & & & & \frac{V_{r_4}}{V_4} & \frac{V_{m_4}}{V_4} & 0 & 0 \end{bmatrix} \begin{bmatrix} \Delta V_{r_2} \\ \Delta V_{m_2} \\ \Delta P_2 \\ \Delta Q_2 \\ \Delta V_{r_3} \\ \Delta V_{m_3} \\ \Delta P_3 \\ \Delta Q_3 \\ \Delta V_{r_4} \\ \Delta V_{m_4} \\ \Delta P_4 \\ \Delta Q_4 \end{bmatrix} \tag{53}$$

The implementation procedure is similar to that used for the conventional PV bus. Instead of using the voltage constraint equation either one of Eqs. (51) and (52) is used depending on the synchronous machine operating point.

6.1. Illustration example

In Fig. 1, suppose the reactive power generation limits are considered for the synchronous machine connected at bus 4, by assuming that the bus 3 is PQ type. The linear system of equations related to the solution algorithm step 1, presented in Ref. [8], is given by Eq. (53).

If the reactive power generation at bus 4 violates either the maximum or minimum limits, the linear system of equations related to the solution algorithm step 1, presented in Ref. [8], is given by Eq. (54).

7. Computational aspects

The proposed formulation, by using the current injection method written in rectangular coordinates, has the same convergence characteristics of the conventional power flow expressed in terms of power mismatches and written in polar coordinates. This formulation has the advantage of presenting a highly sparse structure (augmented Jacobian) suitable to the incorporation of FACTS devices and control of any kind [8]. It is also very important to notice that in the absence of control devices this formulation can be reduced to a $(2n \times 2n)$ formulation as presented in Ref. [12]. As shown in Ref. [12], the saving cpu time for the current injection method is about 20% when compared to the conventional power flow formulation.

The main advantage of this formulation lies on the calculation of the matrix $\mathbf{Y}^*$, because its off-diagonal elements are exactly the terms of admittance matrix bus and the diagonal elements are calculated using non-transcendental functions, even if load models other than constant power are included.

8. Results

The proposed power flow control models were validated through tests with the IEEE-118 buses and the Brazilian South–Southeastern system. These systems have 118 buses

and 186 circuits, and 1768 buses and 2527 circuits, respectively.

8.1. IEEE-118 buses system

In order to validate the secondary voltage control model, the generators at buses 74 and 76 were set to control the voltage at the bus 75, in such a way that $Q_{G_{(76)}} = 2.333 Q_{G_{(74)}}$. The power flow solution was achieved in three iterations with power mismatch less than 1.0×10^{-10} p.u. The results of this simulation are shown in Table 1.

$$
\begin{bmatrix} 0 \\ 0 \\ \Delta P_2 \\ \Delta Q_2 \\ 0 \\ 0 \\ \Delta P_3 \\ \Delta Q_3 \\ 0 \\ 0 \\ \Delta P_4 \\ \Delta Q_4'' \end{bmatrix} =
\begin{bmatrix}
B'_{22} & G'_{22} & \frac{-V_{m_2}}{V_2^2} & \frac{V_{r_2}}{V_2^2} & B_{23} & G_{23} & 0 & 0 & B_{24} & G_{24} & 0 & 0 \\
G''_{22} & B''_{22} & \frac{-V_{r_2}}{V_2^2} & \frac{-V_{m_2}}{V_2^2} & G_{23} & -B_{23} & 0 & 0 & G_{24} & -B_{24} & 0 & 0 \\
0 & 0 & 1 & 0 & 0 & 0 & 0 & 0 & 0 & 0 & 0 & 0 \\
0 & 0 & 0 & 1 & 0 & 0 & 0 & 0 & 0 & 0 & 0 & 0 \\
B_{32} & G_{32} & 0 & 0 & B'_{33} & G'_{33} & \frac{-V_{m_3}}{V_3^2} & \frac{V_{r_3}}{V_3^2} & & & & \\
G_{32} & -B_{32} & 0 & 0 & G''_{33} & B''_{33} & \frac{-V_{r_3}}{V_3^2} & \frac{-V_{m_3}}{V_3^2} & & & & \\
0 & 0 & 0 & 0 & 0 & 0 & 1 & 0 & & & & \\
0 & 0 & 0 & 0 & 0 & 0 & 0 & 1 & & & & \\
B_{42} & G_{42} & 0 & 0 & & & & & B'_{44} & G'_{44} & \frac{-V_{m_4}}{V_4^2} & \frac{V_{r_4}}{V_4^2} \\
G_{42} & -B_{42} & 0 & 0 & & & & & G''_{44} & B''_{44} & \frac{-V_{r_4}}{V_4^2} & \frac{-V_{m_4}}{V_4^2} \\
0 & 0 & 0 & 0 & & & & & 0 & 0 & 1 & 0 \\
0 & 0 & 0 & 0 & & & & & 0 & 0 & 0 & -1
\end{bmatrix}
\begin{bmatrix} \Delta V_{r_2} \\ \Delta V_{m_2} \\ \Delta P_2 \\ \Delta Q_2 \\ \Delta V_{r_3} \\ \Delta V_{m_3} \\ \Delta P_3 \\ \Delta Q_3 \\ \Delta V_{r_4} \\ \Delta V_{m_4} \\ \Delta P_4 \\ \Delta Q_4 \end{bmatrix} \tag{54}
$$

A SVC was included at the bus 93 in order to control the voltage at the bus 102. This SVC was modeled by the reference voltage (V_0) equal to 1.00 p.u. and reactance slope equal to 2%. Two kind of simulations were made, in the first one, the maximum and minimum reactive generation ($Q_G^{\max}, Q_G^{\min}$) were set to be, respectively, 40.0 and −40.0 MVAr, and in the second simulation, the limits of the reactive generation were set to be 50 and −50 MVAr. Table 2 illustrates the results of these simulations, in both cases the convergence was obtained in two iterations with power mismatch less than 1.0×10^{-5} p.u. Note that with reactive generation limits equal to 40.0 MVAr the SVC operates as a capacitor.

For validating the TCSC model, a TCSC was placed between the buses 50 and 57 with the objective of controlling the active power flow between these buses. Table 3 shows the results of three different situations, without TCSC (base case), and with TCSC controlling the power flow between the buses 50 and 57 in 40.0 and 50.0 MW. In all simulations the initial reactance was 9.66% (equal to the base case). The convergence without TCSC was obtained in two iterations and with TCSC was achieved in four iterations with power mismatch less than 1.0×10^{-5} p.u. in all simulations.

Table 1
Power flow solution, IEEE-118: two *P* buses controlling one *PQV* bus

P buses			*PQV* bus		
Number	Generation (MVAr)	Generation (%)	Number	Voltage magnitude	Specified voltage
74	43.54	30	75	1.000	1.000
76	101.59	70	75	1.000	1.000

8.2. Brazilian South–Southeastern system

It was considered a set of twelve *P* buses controlling eleven *PQV* buses, in order to validate the remote voltage control and secondary voltage control models. Each *PQV* bus has its voltage magnitude controlled by a unique *P* bus, except for the 483 bus that was controlled by 403 and 404 buses, in such a way that $Q_{G_{(404)}} = 1.50 Q_{G_{(403)}}$. The power flow solution obtained in five iterations and with power mismatch less than 1.0×10^{-8} p.u. is shown in Tables 4 and 5.

A TCSC was placed between buses 958 and 2750 with the objective of controlling the active power flow between these buses in 32.29 MW. For this control the initial line reactance was the same of the base case and the convergence characteristics was achieved in five iterations when the absolute value of the difference between the specified and calculated active power flow was less than

Table 2
Power flow solution, IEEE-118: SVC

SVC bus					PQV Bus		
Num.	Slope (%)	Limits (MVAr)	Generation (MVAr)	Operation range	Num.	Calculated voltage	Reference voltage (V_0)
93	2.0	40.0	40.50	Capacitive	102	0.9916	1.000
93	2.0	50.0	41.97	Linear	102	0.9916	1.000

Table 3
Power flow solution, IEEE-118: TCSC

Case	Bus		Reactance (%)			Active power flow	
	To	From	Initial	Final	Compensation	MW	Specified MW
No TCSC	50	57	9.660	9.660	–	35.882	–
With TCSC	50	57	9.660	9.541	0.119	40.000	40.0
With TCSC	50	57	9.660	2.503	7.157	50.000	50.0

1.0×10^{-7} p.u. The results from the solution of the power flow, with TCSC and with no TCSC are shown in Table 6.

It was included a SVC at bus 856 for controlling the voltage magnitude at bus 1060, to validate the proposed model for the static voltage compensator. This SVC was modeled by the reference voltage (V_0) equal to 1.00 p.u., and the maximum and minimum reactive generation (Q_G^{max}, Q_G^{min}) equal to 0.75 and -0.75 p.u., respectively. Two different situations were simulated corresponding to the slope reactance (r) equal to 2% (simulation I) and 5% (simulation II). The results related to these simulations are shown in Table 7, where the convergence characteristics were achieved in five iterations, with the active and reactive power mismatch less than 1.0×10^{-7} p.u. in both simulations.

Table 4
Power flow solution, Brazilian South–Southeastern system: *P* and *PQV* buses

P buses		*PQV* buses		
Number	Generation (MVAr)	Number	Voltage magnitude	Specified voltage
28	49.775	190	1.020	1.020
42	−70.351	211	1.000	1.000
44	98.504	178	1.010	1.010
45	−5.7751	151	1.000	1.000
48	−1296.6	86	1.010	1.010
55	−24.524	215	1.000	1.000
389	−60.063	386	1.010	1.010
400	130.41	481	0.977	0.977
401	−60.603	480	0.995	0.995
1500	−8.2745	1526	1.020	1.020

Table 5
Power flow solution, Brazilian South–Southeastern system: two *P* buses controlling one *PQV* bus

P buses			*PQV* bus		
Number	Generation (MVAr)	Generation (%)	Number	Voltage magnitude	Specified voltage
403	69.011	40	483	0.9780	0.9780
404	103.52	60	483	0.9780	0.9780

Table 6
Power flow solution, Brazilian South–Southeastern system: TCSC

Case	Bus		Reactance (%)			Active power flow	
	To	From	Initial	Final	Compensation	MW	Specified MW
No TCSC	958	2750	6.120	6.120	–	26.911	–
With TCSC	958	2750	6.120	0.877	5.243	32.290	32.290

Table 7
Power flow solution, Brazilian South–Southeastern system: SVC

SVC bus			*PQV* bus		
Number	Slope (%)	Generation (MVAr)	Number	Calculated voltage	Reference voltage (V_0)
856	2.0	46.200	1060	0.99076	0.997
856	5.0	19.819	1060	0.99009	0.997

Table 8
Power flow solution, Brazilian South–Southeastern system: reactive limits at a generation bus

PV bus	Reactive generation (MVAr)			Voltage magnitude (p.u.)		
Reactive power load (MVAr)	Proposed formulation	Conventional formulation	No reactive power limits	Proposed formulation	Conventional formulation	No reactive power limits
−20.0	−17,674	−17,300	−39,642	1,0304	1,0377	1,0100
−10.0	−17,519	−17,300	−29,642	1,0213	1,0287	1,0100
00.0	−17,362	−17,300	−19,642	1,0122	1,0195	1,0100
10.0	−9,6423	−9,6423	−9,6423	1,0100	1,0100	1,0100
20.0	0,3577	0,3577	0,3577	1,0100	1,0100	1,0100
30.0	10,358	17,300	10,358	1,0100	0,9909	1,0100
40.0	17,275	17,300	20,358	1,0071	0,9809	1,0100
50.0	17,107	17,300	30,358	0,9973	0,9707	1,0100
60.0	16,936	17,300	40,358	0,9873	0,9603	1,0100

The objective of these last simulations was to compare the results obtained by using the conventional procedure for the *PV* bus with those obtained by considering the proposed formulation in which the reactive power limits are voltage dependent. For this purpose the generator connected at bus 2052 is studied. The nominal values adopted for the power factor and the voltage at this generator bus are 0.85 and 1.010 p.u., respectively. The active power generation is adopted equal to zero, while the apparent power generation is 0.165 p.u. The value of x_q was set to 2% and the resistance set to zero. The maximum continuous stator and rotor currents were set 5 and 10% above respective nominal value and the maximum load angle was set to 80°. In the conventional procedure the minimum and maximum reactive power limits for the 2052 bus were fixed with the values set to −17.3 and +17.3 MVAr.

The results for several values of the reactive power load for each formulation plus the simulations with no reactive power limits are shown in Table 8. These results shown that the proposed formulation presents violated voltages closer of the specified for the problem than the conventional formulation. The convergence characteristics in the both formulation were achieved in six or seven iterations with absolute power flow mismatch less than 1.0×10^{-7} p.u.

9. Conclusions

The augmented formulation is equivalent to the conventional Newton–Raphson power flow regarding convergence characteristics, but allows an easier incorporation of control device models and power flow controls of any kind. This formulation also directly incorporates more realistic modeling of power system components, such as, static var compensators, TCSC and voltage control through multiple reactive sources.

The studies performed so far indicate the proposed formulation may become a valuable tool for solving present

day power flow problems, where the proper consideration of controls is becoming a key issue.

References

[1] Ajjarapu V, Christy C. The continuation power flow: a tool for steady state voltage stability analysis. IEEE Trans Power Syst 1992;7(1): 416–23.

[2] Cañizares CA, Alvarado FL. Point of collapse and continuation methods for large ac/dc systems. IEEE Trans Power Syst 1993;8(1): 1–8.

[3] Overbye TJ, Klump RK. Effective calculation of power system low-voltage solutions. IEEE Trans Power Syst 1996;11(1):75–82.

[4] Semlyen A. Fundamental concepts of a Krylov subspace power flow methodology. IEEE Trans Power Syst 1996;11(3):1528–37.

[5] Lof PA, Andersson G, Hill DJ. Voltage dependent reactive power limits for voltage stability studies. IEEE Trans Power Syst 1995; 10(1):220–8.

[6] Gotham DJ, Heydt GT. Power flow control and power flow studies for systems with FACTS devices. IEEE Trans Power Syst 1998;13(1): 60–5.

[7] Fuerte-Esquivel CR, Acha E. A Newton-type algorithm for the control of power flow in electrical power networks. IEEE Trans Power Syst 1997;12(4):1474–80.

[8] Da Costa VM, Pereira JLR, Martins N. An augmented Newton Raphson power flow formulation based on current injections. Int J Electr Power Energy Syst 2001;23(4):305–12.

[9] Alvarado FL, DeMarco CL. Computational tools for planning and operation involving FACTS devices. Proceedings of Workshop on FACTS, Rio de Janeiro, Brazil; November 1995.

[10] Kundur K. Power system stability and control. New York: McGraw-Hill; 1994.

[11] Taylor CW. Power system voltage stability. New York: McGraw-Hill; 1994.

[12] Da Costa VM, Pereira JLR, Martins N. Developments in the Newton Raphson power flow formulation based on current injections. IEEE Trans Power Syst 1999;14(4):1320–6.